

Trajectory tracking for a four rotor mini-aircraft

Salazar-Cruz, S., Palomino, A. and Lozano, R.

Abstract—In this paper, we present a trajectory tracking controller design and its implementation on a mini rotorcraft having four rotors. The dynamic model of the four-rotor rotorcraft is obtained via a Lagrange approach. Trajectory generation algorithm is proposed. The proposed controller is based on Lyapunov analysis using nested saturation control algorithm. Global stability analysis of the closed-loop system is presented. Real-time experiments show that the mini-aircraft is able to track satisfactorily the desired trajectory.

I. INTRODUCTION

In the past few years, many researches have been attracted to the area of automatic control of flying machines. Generally, the control strategies are based on simplified models. These reduced models should however retain the main features of the aerial vehicle. In this paper, we are interested in the design of a relatively simple trajectory tracking algorithm to perform hover and tracking of desired trajectories. Particularly, we are interesting in controlling a mini rotorcraft having four rotors (Fig. 1). In this type of helicopters, the throttle input is the sum of the thrusts of each motor. Pitch movement is obtained by increasing (reducing) the speed of the rear motor while reducing (increasing) the speed of the front motor. The roll movement is obtained similarly using the lateral motors. The yaw movement is obtained by increasing (decreasing) the speed of the front and rear motors while decreasing (increasing) the speed of the lateral motors. This should be done while keeping the total thrust constant. In this paper, we present the model of

the four-rotor rotorcraft whose dynamical model is obtained via a Lagrange approach [1]. A control strategy is proposed for stabilizing the rotorcraft at hover. Indeed, we first design a control to stabilize the yaw angular displacement and the altitude. We then control the roll angle and the horizontal displacement in the y -axis. Finally, we control the pitch angle and the vertical displacement in the x -axis. The control algorithm is based on the nested saturation control strategy proposed by [10]. We prove global stability of the closed loop system by the Lyapunov method. Furthermore, the proposed controller has been implemented on a real time experimental setup using a mini rotorcraft Draganfly III and a 3D tracker system as an orientations and position sensor. The experimental results show that the proposed control strategy performs well in practice.

II. MODELING

In this section we present the model of a four-rotor rotorcraft using a Lagrangian approach. The generalized coordinates describing the rotorcraft position and orientation are

$$q = (x \ y \ z \ \psi \ \theta \ \phi)^T \quad (1)$$

where (x, y, z) denote the position of the center of mass of the aircraft to the frame I , and (ψ, θ, ϕ) are the three Euler angles (yaw, pitch and roll angles) and represent the orientation of the rotorcraft. Therefore, the model partitions naturally into translational and rotational coordinates as $\xi = (x \ y \ z)^T \in R^3$ and $\eta = (\psi \ \theta \ \phi)^T \in R^3$. The translational kinetic energy of the rotorcraft is $T_{tra} = \frac{1}{2}m\dot{\xi}^T \dot{\xi}$ where m denotes the mass of the rotorcraft. The rotational kinetic energy is $T_{rot} = \frac{1}{2}\dot{\eta}^T J \dot{\eta}$. Here, the matrix J acts as the inertial matrix for the full rotational kinetic energy of the rotorcraft expressed directly in terms of the generalized coordinates η . The only potential energy which needs to be considered is the standard gravitational potential given by $U = mgz$. The Lagrangian is represented by $L = T_{tra} + T_{rot} - U$. Then, we obtain

$$L = \frac{1}{2} \left(m \dot{\xi}^T \dot{\xi} + \dot{\eta}^T J \dot{\eta} - 2mgz \right) \quad (2)$$

The model of the full rotorcraft dynamics is obtained from the Euler-Lagrange equations with external generalized force F and generalized moment τ where F_ξ is the translational force applied to the rotorcraft due to the control input. Then write $\hat{F} = [0 \ 0 \ u]^T$ and

$$u = f_1 + f_2 + f_3 + f_4 \quad (3)$$

where $f_i = k_i \omega_i^2 \quad \forall i = 1, \dots, 4$, $k_i > 0$ is a constant and ω_i is the angular speed of motor i . Therefore $F_\xi =$

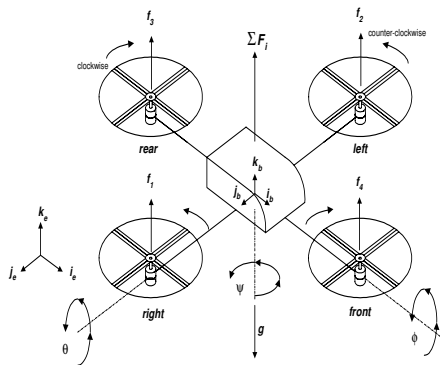


Fig. 1. The four rotor rotorcraft

Heudiasyc-UTC UMR 6599 Centre de Recherches de Royallieu B.P. 20529 60205 Compiègne France Tel.: + 33 (0)3 44 23 44 23 ; fax: +33 (0)3 44 23 44 77

Corresponding author rlozano@hds.utc.fr
sergio@hds.utc.fr
apalomino@hds.utc.fr

$R\hat{F}$ where R is the transformation matrix representing the orientation of the rotorcraft. Now, by simplicity, we use c_θ and s_θ for $\cos \theta$ and $\sin \theta$ respectively, so we have

$$R = \begin{pmatrix} c_\theta c_\psi & s_\psi c_\theta & -s_\theta \\ c_\psi s_\theta s_\phi - s_\psi c_\phi & s_\psi s_\theta s_\phi + c_\psi c_\phi & c_\theta s_\phi \\ c_\psi s_\theta c_\phi + s_\psi c_\phi & s_\psi s_\theta c_\phi - c_\psi c_\phi & c_\theta c_\phi \end{pmatrix}$$

The generalized moments on the η variables are denoted by $\tau = [\tau_\phi \ \tau_\theta \ \tau_\psi]^T$ where

$$\begin{aligned} \tau_\phi &= (f_3 - f_1) l \\ \tau_\theta &= (f_2 - f_4) l \\ \tau_\psi &= \sum_{i=1}^4 \tau M_i \end{aligned} \quad (4)$$

where l is the distance to the center of gravity and τM_i is the couple produced by the motor M_i . Since the Lagrangian contains no cross terms in the kinetic energy, combining ξ and η , the Euler-Lagrange equation can be partitioned into the dynamics for the ξ coordinates and the η dynamics. So, we obtain

$$\begin{aligned} m\ddot{\xi} + mg\mathbf{z} &= F_\xi \\ J\ddot{\eta} + \dot{J}\dot{\eta} - \frac{1}{2} \frac{\partial}{\partial \eta} (\dot{\eta}^T J \dot{\eta}) &= \tau \end{aligned} \quad (5)$$

Defining the Coriolis terms and gyroscopic and centrifugal terms as

$$C(\eta, \dot{\eta}) \dot{\eta} \triangleq \dot{J}\dot{\eta} - \frac{1}{2} \frac{\partial}{\partial \eta} (\dot{\eta}^T J \dot{\eta}) \quad (6)$$

Finally we obtain

$$\begin{aligned} m\ddot{\xi} &= u \begin{bmatrix} -s_\theta \\ c_\theta s_\phi \\ c_\theta c_\phi \end{bmatrix} + \begin{bmatrix} 0 \\ 0 \\ -mg \end{bmatrix} \\ J\ddot{\eta} &= -C(\eta, \dot{\eta}) \dot{\eta} + \tau \end{aligned} \quad (7)$$

III. TRAJECTORY GENERATION

We define a polynomial smooth curve as the desired y^d trajectory of the quad-rotor

$$y^d(t) \triangleq a_0 + a_1 t + a_2 t^2 + a_3 t^3 \quad (8)$$

Then the desired velocity is automatically given as

$$\dot{y}^d(t) = a_1 + 2a_2 t + 3a_3 t^2 \quad (9)$$

and

$$\begin{aligned} \ddot{y}^d(t) &= 2a_2 + 6a_3 t \\ y^{(3)d}(t) &= 6a_3 \end{aligned} \quad (10)$$

We choose the trajectory initial conditions so that $a_0 = 0$, $a_1 = 0$, $a_2 = \frac{3L}{t_f^2}$ and $a_3 = -\frac{2L}{t_f^3}$ where L is the length of the path and t_f the total final time.

IV. NONLINEAR CONTROL LAW WITH NESTED SATURATIONS

In this section we will develop a control strategy for stabilizing the rotorcraft at hover. We will prove global stability of the closed loop system. Furthermore, the proposed controller design is such that the resulting controller is relatively simple and each of the control inputs can operate in either manual or automatic mode independently. The collective input u in (7) is essentially used to make the altitude reach a desired value. The control input τ_ψ is used to set the yaw displacement to zero, τ_θ is used to control the pitch and the horizontal movement in the x -axis. Similarly τ_ϕ is used to control the roll and horizontal displacement in the y -axis. In order to simplify, let us propose a change of the input variables

$$\tau = J\tilde{\tau} + C(\eta, \dot{\eta}) \dot{\eta} \quad (11)$$

where

$$\tilde{\tau} = [\tilde{\tau}_\phi \ \tilde{\tau}_\theta \ \tilde{\tau}_\psi]^T \quad (12)$$

So, rewriting equation (7) we have

$$\begin{aligned} m\ddot{x} &= -u \sin \theta \\ m\ddot{y} &= u \cos \theta \sin \phi \\ m\ddot{z} &= u \cos \theta \cos \phi - mg \\ \ddot{\phi} &= \tilde{\tau}_\phi \\ \ddot{\theta} &= \tilde{\tau}_\theta \\ \ddot{\psi} &= \tilde{\tau}_\psi \end{aligned} \quad (13)$$

where x and y are the coordinates in the horizontal plane, and z is the vertical position, ψ is the yaw angle around the z -axis, θ is the pitch angle around the y -axis, and ϕ is the roll angle around the x -axis. The control inputs u , $\tilde{\tau}_\phi$, $\tilde{\tau}_\theta$ and $\tilde{\tau}_\psi$ are the total thrust or collective input (directed out the bottom of the aircraft) and the angular moments, respectively.

A. Altitude and yaw control

The control of the vertical position can be obtained by using the following control input

$$u = \frac{(r_1 + mg)}{c_\theta c_\phi} \quad (14)$$

where

$$r_1 = -a_{z_1} \dot{z} - a_{z_2} (z - z_d) \quad (15)$$

here, a_{z_1} , a_{z_2} are positive constants and z_d is the desired altitude. The yaw angular position can be controlled by applying

$$\tilde{\tau}_\psi = -a_{\psi_1} \dot{\psi} - a_{\psi_2} (\psi - \psi_d) \quad (16)$$

Provided that $c_\theta c_\phi \neq 0$, we obtain

$$\begin{aligned} m\ddot{x} &= -\frac{(r_1 + mg)}{c_\phi} \tan \theta \\ m\ddot{y} &= (r_1 + mg) \tan \phi \\ m\ddot{z} &= -a_{z_1} \dot{z} - a_{z_2} (z - z_d) \\ \ddot{\phi} &= \tilde{\tau}_\phi \\ \ddot{\theta} &= \tilde{\tau}_\theta \\ \ddot{\psi} &= -a_{\psi_1} \dot{\psi} - a_{\psi_2} (\psi - \psi_d) \end{aligned} \quad (17)$$

The control parameters a_{ψ_1} , a_{ψ_2} , a_{z_1} and a_{z_2} are chosen to ensure a stable well-damped response in the vertical and yaw axes.

B. Roll and y Control Trajectory

Note that, from (15) and (17), $r_1 \rightarrow 0$ for a time T large enough; r_1 and ψ are arbitrarily small, therefore the subsystem x and y (see (17)) reduces to

$$\ddot{x} = -g \frac{\tan \theta}{\cos \phi} \quad (18)$$

$$\ddot{y} = g \tan \phi \quad (19)$$

We will first consider the subsystem ϕ given by (17) and (19). We will implement a non-linear controller design based on nested saturations. This type of control allows in the limit to guarantee arbitrary bounds for ϕ , $\dot{\phi}$, e_y and \dot{e}_y . To further simplify the analysis, we will impose a very small upper bound on $|\phi|$ in such a way that the difference $\tan \phi - \phi$ is arbitrarily small. Rewriting (17) and (19) we get:

$$\ddot{y} = g\phi \quad (20)$$

and

$$\ddot{\phi} = \tilde{\tau}_\phi \quad (21)$$

then

$$y^{iv} = g\tilde{\tau}_\phi \quad (22)$$

which represents four integrators in cascade. We define

$$e_y \triangleq \frac{1}{g} (y - y^d) \quad (23)$$

then

$$\dot{e}_y = \frac{1}{g} (\dot{y} - \dot{y}^d) \quad (24)$$

$$\ddot{e}_y = \frac{1}{g} (\ddot{y} - \ddot{y}^d) = \left(\phi - \frac{1}{g} \ddot{y}^d \right)$$

$$e_y^{(3)} = \frac{1}{g} (\dot{y}^{(3)} - \dot{y}^{(3)d}) = \left(\dot{\phi} - \frac{1}{g} \dot{y}^{(3)d} \right)$$

$$e_y^{(4)} = \ddot{\phi}$$

Then, we propose

$$\tilde{\tau}_\phi = -\sigma_{\phi_1} \left(e_y^{(3)} + \sigma_{\phi_2} (\zeta_{\phi_1}) \right) \quad (25)$$

where $\sigma_i(s)$ is a saturation function such that $|\sigma_i(s)| \leq M_i$ for $i = 1, 2, \dots$ and ζ_{ϕ_1} will be defined later to ensure global stability. We propose the following positive function

$$V = \frac{1}{2} \left(e_y^{(3)} \right)^2 \quad (26)$$

Then from the equations (24) and (25) we have $\dot{V} = -e_y^{(3)} \sigma_{\phi_1} (e_y^{(3)} + \sigma_{\phi_2} (\zeta_{\phi_1}))$. Note that if $|e_y^{(3)}| > M_{\phi_2}$, then $\dot{V} < 0$, this means that there exists T_1 such that $|e_y^{(3)}| \leq M_{\phi_2}$ for $t > T_1$. Now, let us define the variable ν_1 as follows

$$\nu_1 \triangleq e_y^{(3)} + \ddot{e}_y \quad (27)$$

Differentiating

$$\dot{\nu}_1 = \dot{e}_y^{(3)} - \sigma_{\phi_1} \left(e_y^{(3)} + \sigma_{\phi_2} (\zeta_{\phi_1}) \right) \quad (28)$$

Let us choose

$$M_{\phi_1} \geq 2M_{\phi_2} \quad (29)$$

From the definition of $\sigma(s)$, we can see that $|\sigma_i(s)| \leq M_i$ for $i = 1, 2, \dots$. This implies that in a finite time, there exists a time T_1 such that $|e_y^{(3)}| \leq M_{\phi_2}$ for $t \leq T_1$. Therefore, for $t \leq T_1$, $|e_y^{(3)} + \sigma_{\phi_2} (\zeta_{\phi_1})| \leq 2M_{\phi_2}$. It then follows that for $t \geq T_1$

$$\sigma_{\phi_1} \left(e_y^{(3)} + \sigma_{\phi_2} (\zeta_{\phi_1}) \right) = e_y^{(3)} + \sigma_{\phi_2} (\zeta_{\phi_1}) \quad (30)$$

Using (28) and (30) we get

$$\dot{\nu}_1 = -\sigma_{\phi_2} (\zeta_{\phi_1}) \quad (31)$$

Let us define

$$\zeta_{\phi_1} \triangleq \nu_1 + \sigma_{\phi_3} (\zeta_{\phi_2}) \quad (32)$$

Introducing the above in (31), it follows

$$\dot{\nu}_1 = -\sigma_{\phi_2} (\nu_1 + \sigma_{\phi_3} (\zeta_{\phi_2})) \quad (33)$$

The upper bounds are assumed to satisfy the following condition

$$M_{\phi_2} \geq 2M_{\phi_3} \quad (34)$$

This implies that there exists a time T_2 such that $|\nu_1| \leq M_{\phi_3}$ for $t \leq T_2$. From (33) and (34), we have that for $t \geq T_2$, $|\nu_1 + \sigma_{\phi_3} (\zeta_{\phi_2})| \leq 2M_{\phi_3}$. It then follows that, for $t \geq T_2$

$$\sigma_{\phi_2} (\nu_1 + \sigma_{\phi_3} (\zeta_{\phi_2})) = \nu_1 + \sigma_{\phi_3} (\zeta_{\phi_2}) \quad (35)$$

Let us define

$$\nu_2 \triangleq \nu_1 + \ddot{e}_y + \dot{e}_y \quad (36)$$

Differentiating, we obtain

$$\dot{\nu}_2 = \dot{\nu}_1 + e_y^{(3)} + \ddot{e}_y \quad (37)$$

Using (27), (33) and (35) into (37), we obtain

$$\dot{\nu}_2 = -\sigma_{\phi_3} (\zeta_{\phi_2}) \quad (38)$$

Now, let us define ζ_{ϕ_2} as

$$\zeta_{\phi_2} \triangleq \nu_2 + \sigma_{\phi_4} (\zeta_{\phi_3}) \quad (39)$$

So, we can rewrite (38) as

$$\dot{\nu}_2 = -\sigma_{\phi_3}(\nu_2 + \sigma_{\phi_4}(\zeta_{\phi_3})) \quad (40)$$

If we chose

$$M_{\phi_3} \geq 2M_{\phi_4} \quad (41)$$

then we conclude that in a finite time, there exists a time T_3 such that $|\nu_2| \leq M_{\phi_4}$ for $t \geq T_3$. Now, for $t \geq T_3$, $|\nu_2 + \sigma_{\phi_4}(\zeta_{\phi_3})| \leq 2M_{\phi_4}$. It then follows that,

$$\sigma_{\phi_3}(\nu_2 + \sigma_{\phi_4}(\zeta_{\phi_3})) = \nu_2 + \sigma_{\phi_4}(\zeta_{\phi_3}) \quad (42)$$

Defining

$$\nu_3 \triangleq \nu_2 + \ddot{e}_y + 2\dot{e}_y + e_y \quad (43)$$

and differentiating we get

$$\dot{\nu}_3 = \dot{\nu}_2 + e_y^{(3)} + 2\ddot{e}_y + \dot{e}_y \quad (44)$$

Finally, using (27), (36), (40) and (42) into (44), we obtain

$$\dot{\nu}_3 = -\sigma_{\phi_4}(\zeta_{\phi_3}) \quad (45)$$

We propose ζ_{ϕ_3} of the following form

$$\zeta_{\phi_3} \triangleq \nu_3 \quad (46)$$

then we have

$$\dot{\nu}_3 = -\sigma_{\phi_4}(\nu_3) \quad (47)$$

This implies that $\nu_3 \rightarrow 0$ as $t \rightarrow \infty$. From (40) it follows that $\nu_2 \rightarrow 0$ and from equation (39), $\zeta_{\phi_2} \rightarrow 0$. From (33), $\nu_1 \rightarrow 0$ then, from (32), $\zeta_{\phi_1} \rightarrow 0$. We can see from equation (??) that $e_y^{(3)} \rightarrow 0$. It follows that from equation (27), we get $\dot{e}_y \rightarrow 0$. Then, from (36), $e_y \rightarrow 0$ and finally from (43), $e_y \rightarrow 0$. Using (27), (32), (36), (39), (43) and (46), we can rewrite equation (25) as

$$\begin{aligned} \tilde{\tau}_\phi &= -\sigma_{\phi_1}(e_y^{(3)} + \sigma_{\phi_2}(e_y^{(3)} + \ddot{e}_y) \\ &\quad + \sigma_{\phi_3}(e_y^{(3)} + 2\ddot{e}_y + \dot{e}_y) \\ &\quad + \sigma_{\phi_4}(e_y^{(3)} + 2\ddot{e}_y + 2\dot{e}_y + e_y)) \end{aligned} \quad (48)$$

C. Pitch and x control trajectory

In the previous section, we obtained $\phi \rightarrow 0$, so we have

$$\ddot{x} = -g \tan \theta \quad (49)$$

Then, we take the sub-system

$$\begin{aligned} \dot{x} &= -g \tan \theta \\ \dot{\theta} &= \tilde{\tau}_\theta \end{aligned} \quad (50)$$

We assume that the control strategy will insure a very small bound on $|\theta|$ in such a way that $\tan \theta \approx \theta$. Therefore the subsystem given in (50), reduces to

$$\begin{aligned} \dot{x} &= -g\theta \\ \dot{\theta} &= \tilde{\tau}_\theta \end{aligned}$$

Using the same procedure to the roll control with $e_x \triangleq \frac{1}{g}(x - x^d)$ and $x^d(t) = b_0 + b_1t + b_2t^2 + b_3t^3$, we have finally get

$$\begin{aligned} \tilde{\tau}_\theta &= -\sigma_{\theta_1}(-e_x^{(3)} + \sigma_{\theta_2}(-\ddot{e}_x \\ &\quad + \sigma_{\theta_3}(-\ddot{e}_x - \dot{e}_x + \\ &\quad \sigma_{\theta_4}(-2\ddot{e}_x - 2\dot{e}_x - e_x))) \end{aligned} \quad (51)$$

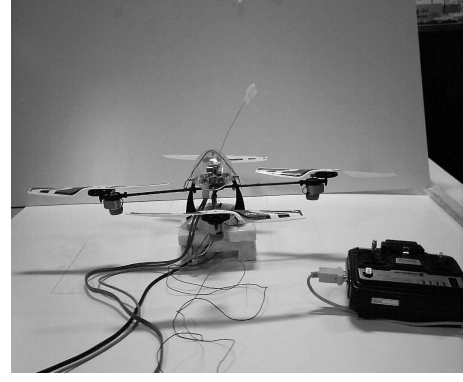


Fig. 2. The minirotorcraft Draganfly III

Phase	Control parameter	Value
Altitude	a_{z1}	0.2
	a_{z2}	0.01
Yaw control	$a_{\varphi 1}$	1.3
	$a_{\varphi 2}$	0.4
Roll control	$M_{\phi 1}$	8
	$M_{\phi 2}$	4
	$M_{\phi 3}$	2
	$M_{\phi 4}$	1
Pitch control	$M_{\theta 1}$	8
	$M_{\theta 2}$	4
	$M_{\theta 3}$	2
	$M_{\theta 4}$	1
Sample	T	$\frac{1}{20}$ s

V. REAL-TIME EXPERIMENTS

In this section we present the results obtained when applying the control strategy proposed in the non linear control section. We are using a minirotorcraft Draganfly III (see Figure 2). We are using a Futaba Skysport 4 radio for transmitting the control signals. These control signals are constrained in the radio to satisfy $1.1V < u < 4.70V$ and $0.66V < \tau_i < 4.16V$. We are using MATLAB SIMULINK Real-Time Windows Target. The rotorcraft evolves freely in a 3D space without any flying stand. In order to measure the position (x, y, z) and the orientation (ψ, θ, ϕ) of the rotorcraft, we use the 3D tracker system (POLHEMUS) with the sensor long ranger. We have the initial conditions $(x, \dot{x}, y, \dot{y}) = (0, 0, 0, 0)$ and $(\psi, \theta, \phi) = (0, 0, 0)$ and the trajectories are $x^d(t) = 0.208t^2 - 0.00231t^3$ and $y^d(t) = 0.03t^2 - 0.00033t^3$ for $t_f = 60s$. with $L_x = 250$ cm and $L_y = 36$ cm. The gain values for the control law are shown in Table 1. Figures (3)–(13) show the performance of the controller.

VI. CONCLUSIONS

We presented a new trajectory control algorithm for a quad-rotor mini-aircraft with saturation inputs. The control law show that the trajectory error of the quad-rotor converge to zero. The experimental results have shown that the proposed strategy has been successfully applied to the rotorcraft on a real-time setup.

REFERENCES

- [1] Fantoni, I. and Lozano, R. (2001a). *Non-linear control of underactuated mechanical systems*. Communications and Control Engineering Series. Springer-verlag. London.

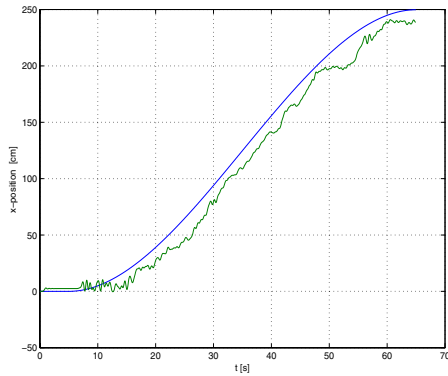


Fig. 3. x-position of the rotorcraft

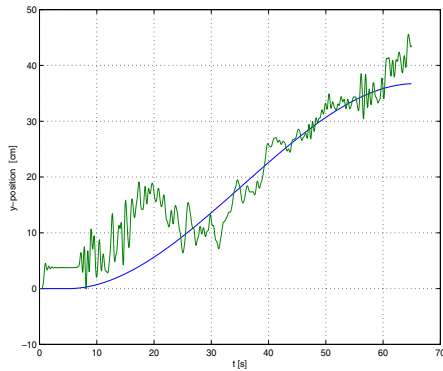


Fig. 4. y-position of the rotorcraft

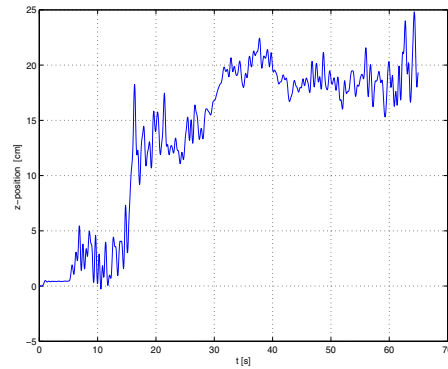


Fig. 5. z-position of the rotorcraft

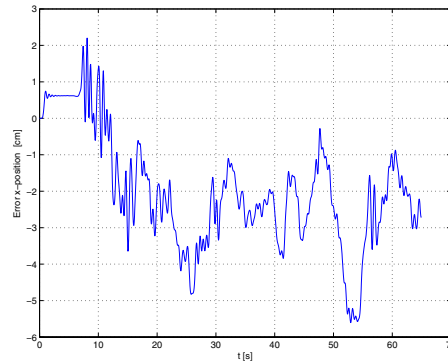


Fig. 6. x error position of the rotorcraft

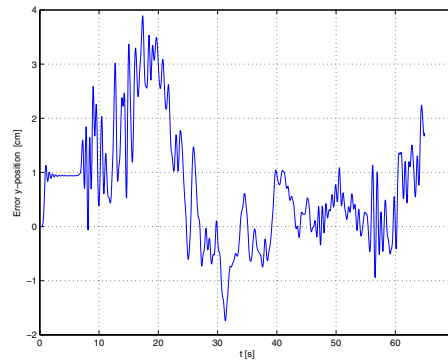


Fig. 7. y error position of the rotorcraft

- [2] Castillo, P., Dzul, A. and Lozano, R. (2004). *Real-time stabilization and tracking of a four rotor mini rotorcraft*. IEEE Transactions on Control Systems Technology, Vol. 12, Number 4, pp. 510-516.
- [3] Dzul, A., Lozano R. and Castillo, P. (2003). *Adaptive altitude control for a small helicopter in a vertical flying stand*. CDC'03, Hawaii, USA, December.
- [4] Fantoni, I. and Lozano, R. (2001b). *Control of nonlinear mechanical systems*. European Journal of Control, Vol. 7, pp. 328-348.
- [5] Etkin, B. (1959). *Dynamics of flight*. John Wiley and Sons, Inc. New York.
- [6] Marconi, L., Isidori, A. and Serrani, A. (2002). *Autonomous vertical landing on oscillating platform: an internal-model based approach*. Automatica, Vol. 38, pp. 21-32.
- [7] Barnes McCormick, W. (1995). *Aerodynamics aeronautics and flight mechanics*. John Wiley and Sons. New York.
- [8] Olfati-Saber, R. (1999). *Global configuration stabilization for the VTOL aircraft with strong input coupling*. In proceedings of the 39th IEEE Conf. on Decision and Control. Sydney, Australia, Dec. 1999.
- [9] Hauser, J., Sastry S. and Meyer, G. (1992). *Nonlinear control design for slightly nonminimum phase systems: Applications to VISTOL aircraft*. Automatica. Vol. 28(4), pp. 665-679.
- [10] Teel, A. R. (1992). *Global stabilization and restricted tracking for multiple integrators with bounded controls*. Systems and Control Letters, Vol. 18, pp. 165-171.
- [11] Tanaka, K., Ohtake, H. and Wang, H. (2004). *A practical design approach to stabilization of a 3-DOF RC helicopter*. Transactions on Automatic Control. Vol. 12(2), pp. 315-325.
- [12] Spong, M. W. and Vidyasagar, M. (1989). *Robot Dynamics and control*. John Wiley and Sons.

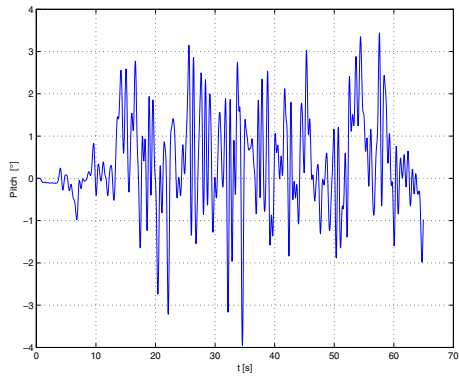


Fig. 8. pitch angle of the rotorcraft

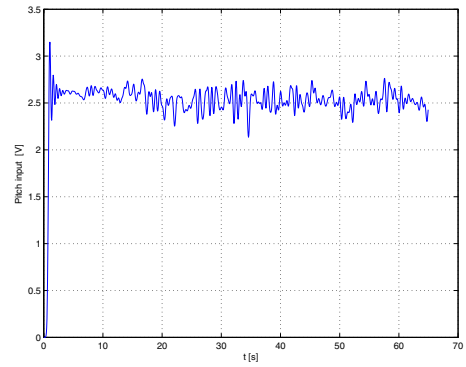


Fig. 11. pitch input of the rotorcraft

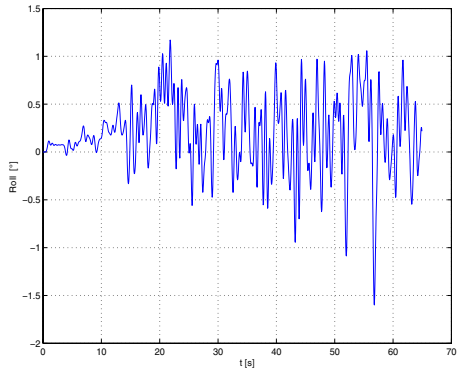


Fig. 9. roll angle of the rotorcraft

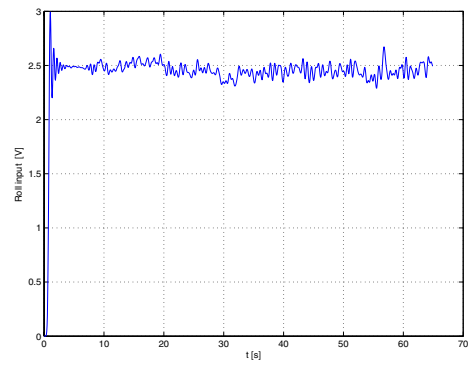


Fig. 12. roll input of the rotorcraft

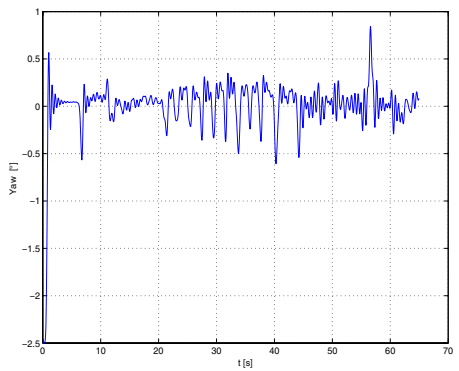


Fig. 10. yaw angle of the rotorcraft

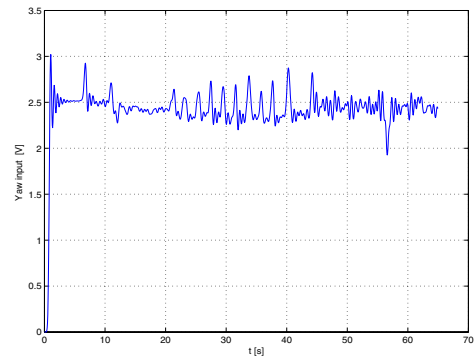


Fig. 13. yaw input of the rotorcraft